J Mol Model (2011) 17:2559–2567
DOI 10.1007/s00894-010-0937-8

ORIGINAL PAPER

In *silico* study on the substrate binding manner in human *myo*-inositol monophosphatase 2

Seisuke Fujita · Tetsuo Ohnishi · Shujiro Okuda · Ryo Kobayashi · Satoshi Fukuno · Daisuke Furuta · Takeshi Kikuchi · Takeo Yoshikawa · Norihisa Fujita

Received: 11 September 2010 / Accepted: 15 December 2010 / Published online: 7 January 2011

Abstract The human IMPA2 gene encoding *myo*-inositol monophosphatase 2 is highly implicated with bipolar disorder but the substrates and the reaction mechanism of *myo*-inositol monophosphatase 2 have not been well elucidated.9 In the present study, we constructed 3D models of three- and two-Mg^{2+}-ion bound *myo*-inositol monophosphatase 2, and studied substrate-binding manners using the docking program AutoDock3. The subsequent study showed that the three-metal-ion model could interact with *myo*-inositol monophosphates, as follows: The phosphate moiety coordinated three Mg^{2+} ions, and the inositol ring formed hydrogen bonds with the amino acids conserved in the family. Furthermore, the OH group vicinal to the phosphate group formed a hydrogen bond with a non-bridging oxygen atom of the phosphate. These interactions have been proposed as crucial for forming the transitional state, bipyramidal structure in the bovine *myo*-inositol monophosphatase. We therefore propose that the human *myo*-inositol monophosphatase 2 interacts with *myo*-inositol monophosphates in the three-metal-ion bound form, and proceeds the dephosphorylation through the three-metal-ion theory.

Keywords AutoDock · Bipolar disorder · Enzyme-substrate docking · Human *myo*-inositol monophosphatase 2 · Three-metal-ion theory

D. Furuta · N. Fujita (✉)
Laboratory of Pharmacoinformatics, School of Pharmacy,
Ritusmeikan University,
Kusatsu, Shiga 525-8577, Japan
e-mail: nori@ph.ritsumei.ac.jp

T. Ohnishi · T. Yoshikawa
Laboratory for Molecular Psychiatry,
RIKEN Brain Science Institute,
Wako, Saitama 351-0198, Japan

S. Fujita · S. Okuda · R. Kobayashi · S. Fukuno · T. Kikuchi
Department of Bioinformatics, College of Information Science and Engineering, Ritsumeikan University,
Kusatsu, Shiga 525-8577, Japan

Introduction

The human IMPA2 gene, which encodes *myo*-inositol monophosphatase 2 (IMPA2) with 288 amino acids, maps on to chromosome 18p11.2, a genetic linkage region for bipolar disorder (also known as manic depression) [1, 2]. In addition, recent studies have shown the genetic association of IMPA2 with bipolar disorder [3, 4]. Interestingly, risk SNPs (single nucleotide polymorphisms) detected in the promoter region of IMPA2 up-regulates its transcriptional activity [3]. In agreement with this result, the transcripts for IMPA2 tend to be higher in postmortem brains from bipolar patients than in those from control subjects. Taken together with that lithium salts are effective in the treatment of bipolar disorder and have been shown to inhibit inositol monophosphatase activity [5, 6], these results suggest the implication of IMPA2 in bipolar disorder. As well as bipolar disorder, chromosome 18p11.2 has also been proposed to include genetic linkage regions for schizophrenia and febrile seizure [7]. On the other hand, as for IMPA1, no genetic evidence has been demonstrated in mental disorders [4].

In contrast to IMPA1, there have been limited numbers of reports studying the biochemical nature of IMPA2. *Myo*-inositol monophosphates, glycerophosphate, glucose-1- phosphate, and 2'-AMP are known to be in vitro substrates for human

IMPA1 but these compounds act as weak substrates for human IMPA2, although the sequence of human IMPA2 shares 54% amino acid identity with that of the human IMPA1.

It still remains enigmatic what is structural basis for the biochemical nature between the two similar enzymes, IMPA1 and IMPA2. Recently, Arai et al. reported four crystal structures of human IMPA2 (crystal 1-4) [8]. These structures are very similar to each other and commonly comprise an α-β protein, with a five-layered sandwich of α -helices and β-sheets (α-β-α-β-α). The overall structure of IMPA2 monomer is similar to that of IMPA1 except for the loop regions (Fig. 1). In IMPA1, the loop region (a.a.31-43) is located at the entrance of the active site cavity. In the corresponding region (a.a.42-54) of IMPA2, the residues are disordered and partially form an α-helix. The structural difference in the opening of the active cavity suggests that the substrate specificity or its binding manner may differ between the IMPA1 and IMPA2.

Greasley and Gore hypothesized in their early work that IMPase operated by a two-metal-ion mechanism [9, 10]. In the theory, the first metal ion may activate water for nucleophilic attack, and a second metal ion, coordinated by three aspartate residues, appears to act as a Lewis acid, stabilizing the leaving inositol oxyanion. However, the two-metal-ion theory has recently been amended to a three-metal-ion theory. Gill et al. reported the bovine IMPA structure in a complex, with the substrate inositol 1-phosphate and three Mg^{2+} ions [11]. The first and second Mg^{2+} ions act in a similar way to the two-metal mechanism. However, in the three metal mechanism, the third metal ion is also carried in by the substrate and, although its binding is weak and not cooperative, it is necessary for the creation of the water nucleophile [11–13]. Metals 1 and 3 constitute a classic homobinuclear center that seems to play a special role in stabilizing the formation of the trigonal bipyramidal transition state. Metal 2 plays an important role for protonation of the leaving inositol moiety by interacting with bridging (ester) oxygen and Asp220 of IMPA1 which corresponds to Asp231 of IMPA2. These three ions were coordinated by the conserved residues, Glu70, Asp90, Asp93 and Asp220. Some of these amino acids contribute to stabilize the intermediate of the enzyme-substrate complex, too [14].

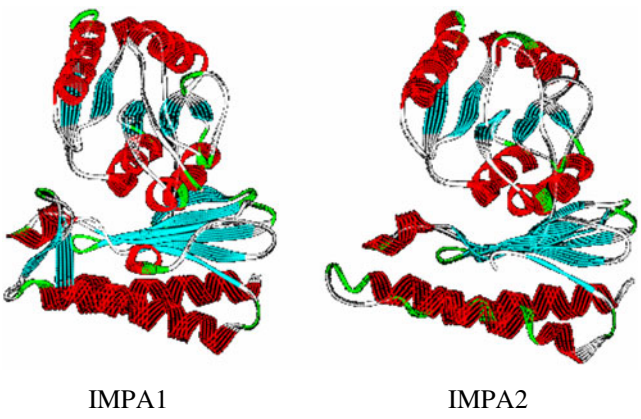

Fig. 1 The crystal structures of human IMPA1 and 2. The figures show the crystal structures of human IMPA1 and 2 that have been reported in the PDB (1awb and 2ddk for IMPA1 and 2, respectively)

The analytical ultracentrifugation of purified human IMPA2 showed that the molecular weight of IMPA2 was 64.9 kDa, while the molecular weight of the IMPA2 monomer was deduced to be 32.4 kDa from the primary sequence. These results indicate that the IMPA2 protein exists as a dimer in solution [8, 15–17]. Although Mg^{2+} ions are required for the enzymatic activity of IMPAs [14–16], an electron density for Mg^{2+} ion was not found in the reported 3D structures of IMPA2-dimer. Only the crystal structure of IMPA2 monomer (PDB-ID;2czi) coordinates two Ca^{2+} ions at the active cavity, while Ca^{2+} is not an activator of IMPase [15]. Therefore, when we conduct docking studies on the substrates to three-metal-ion bound IMPA2, we have to prepare a 3D model of IMPA2-dimer that forms a complex with three Mg^{2+} ions.

In our laboratory, we have obtained practical results in discovering surrogate P2Y receptor ligands [18, 19] using AutoDock3, a docking program developed by Morris' group [20]. The features of this program are that i) a large configuration space can be searched, ii) the perfect flexibility of a ligand molecule can be taken into consideration, and iii) docking is accelerated by calculating the interaction between a protein and a ligand in a grid base. Using these tools, we found the surrogate ligands that bind on the human $P2Y_1$, $P2Y_{10}$, and $P2Y_{12}$ receptors with high affinities [18, 19, 21]. In this paper, we studied the substrate binding manner in human IMPA2 using the docking program and reported the possible reaction mechanism of human IMPA2.

Materials and methods

In silico docking

We used AutoDock3.1, a ligand flexible docking program [20], according to the manufacturer's instructions. The number of grid points in the x, y, z-axis was 60×60 × 60 Å with grid points separated by 0.375 Å. The population size was set to 50. Each docking experiment consisted of a series of 200 simulations. We defined the grid center based on the active site of human IMPA1. The definite grid centers were, x=9.0, y=54.6, z=14.3 for IMPA1 and x= 34.0, y=12.5, and z=6.6 for IMPA2. The phosphate compound database was prepared on the basis of the 2D molecules in the KEGG ligand database (http://www.genome.ad.jp/ligand/). These 2D molecules were converted

to 3D molecules using DS Modeling (Accelrys, San Diego, CA, USA) and energy-minimized with the program CHARMm force field (1000 steps both for the Steepest Descent and Conjugated Gradient algorithms) and molecular dynamics in the conditions; heating at 300 K, 1000 steps by 0.001pS for equilibration and 1000 steps by 0.001pS for leap-frog Verlet integration algorithm.

Construction of the 3D structure of the human IMPA2 in complex with three metal ions

As a positive control study we used the crystal structure of human IMPA1 (PDB-ID;1awb) from which *myo*-inositol phosphate was removed. Three Ca^{2+} ions were originally coordinated in the crystal structure. Using this structure as a template, we conducted a control docking study of the substrates to IMPA1 with AutoDock3.

Although Mg^{2+} ion is known to be required for the enzymatic activity of IMPA1 [22–24] and IMPA2 [15], no crystal structure of three-metal-ion bound IMPA2 has been reported. Therefore, we built a 3D model structure of the human IMPA2 that formed a complex with three Mg^{2+} ions. Based on the 3D structure of human IMPA1, we added three Mg^{2+} ions to the crystal structure of human IMPA2-dimer (PDB entry;2ddk). Mg^{2+}-1 was placed in the site1 surrounded by Glu81, Asp101 and Ile103, and Mg^{2+}-2 was in site2 surrounded by Asp101, Asp104, and Asp231. The third Mg^{2+} ion was bound to Glu81 to form a triangle with other Mg^{2+} ions in a similar way to the IMPA1. The constructed structure was energy-minimized using the program CHARMm force field. For the docking study of the two Mg^{2+} ions-bound IMPA2, we used the model structure that coordinated two Mg^{2+} ions at sites 1 and 2. The parameter for Mg^{2+} was added from the metals parameter set distributed by DS Modeling. Hydrogen atoms were added to the protein using the CHARMm command. Charges were taken from the standard Kollman parameter set for phosphate molecules and protein residues.

For the study of the substrate-docking on the metal free IMPA2, we used the crystal structure of 2ddk as a docking template.

The docking was verified by monitoring the value of free energy change (ΔG) caused by enzyme-substrate docking. The calculation followed the equation given as:

$$\Delta G = \Delta G_{vdw} + \Delta G_{hbond} + \Delta G_{elec} + \Delta G_{tor} + \Delta G_{sol}$$

(http://autodock.scripps.edu/resources/science/equations.)

The standard deviation of ΔG values from a series of 200 docking simulations was calculated to evaluate the reproducibility of the relevant docking. We counted the number of hydrogen bonds formed between each substrate and the conserved amino acids such as Asp104, Arg207, Gln224, and Asp231 of human IMPA2. We investigated the substrate-binding manner precisely, when the number of hydrogen bonds was more than two.

All graphic representations were obtained by DS modeling.

Results and discussion

When we used the crystal structure of human IMPA1 as a template, the docking study showed that 83 of 200 docking results significantly resemble each other and the 83 results were superimposed as shown in Fig. 2a. The r.m.s. deviations of phosphorus atom and C4 were 0.21 and 0.35 Å, respectively.

Their binding manners were unified as follows: Two of three non-bridging oxygen atoms, O8 and O9 of the phosphate group, interacted with three Ca^{2+} ions within 3 Å, and the 2-OH and 4-OH groups of inositol ring formed hydrogen bonds with Asp93 and Glu213, respectively (Fig. 2b). The 6-OH group interacted with Asp220 at a distance of 3.8 Å, and was close to the oxygen O9, which coordinated Ca^{2+}-3 (Fig. 2c). These results are well consistent with those of the crystal structure of IMPA1-inositol 1-phosphate complex (Fig. 2d, e). The average ΔG value produced by the 200 dockings was about -12 kcal mol^{-1}, and the deviation of ΔG values was less than 0.2 (Table 1).

These docking results demonstrate that AutoDock3 can be usable to predict the possible binding manner of IMPA and *myo*-inositol monophosphates. Notably, in the docking models, intermolecular interactions are shown between two non-bridging oxygen atoms and three Ca^{2+} ions, and also the bridging oxygen O1 and Ca^{2+}-2 (Fig. 2b, c). These interactions have been shown to be important for proton transfer to the leaving oxygen O1 group, resulting in phosphate hydrolysis [11, 12]. Furthermore, the 6-OH group of the inositol ring is close to the phosphate oxygen that interacts with Ca^{2+}-3 (Fig. 2c, e). The OH group can work as a hydrogen bond donor that is required in the catalytic mechanism for the hydrolysis in the bovine IMPA [11]. Gill et al. elucidated that in the bovine IMPA, the pentavalent phosphorus transition state is stabilized by coordination to each of the three Mg^{2+} ions and by the hydrogen bond with the 6-OH group, oriented to a position coincident to an active site [11, 12]. Our present docking models are consistent with their proposing mechanism of IMPA-catalyzed dephosphorylation reaction. Thus, we evaluated that AutoDock3 was a very useful tool for predicting the docking manner of *myo*-inositol monophosphates to human IMPA2.

Subsequently, we conducted a docking study on *myo*-inositol monophosphates to the three-Mg^{2+}-ion bound

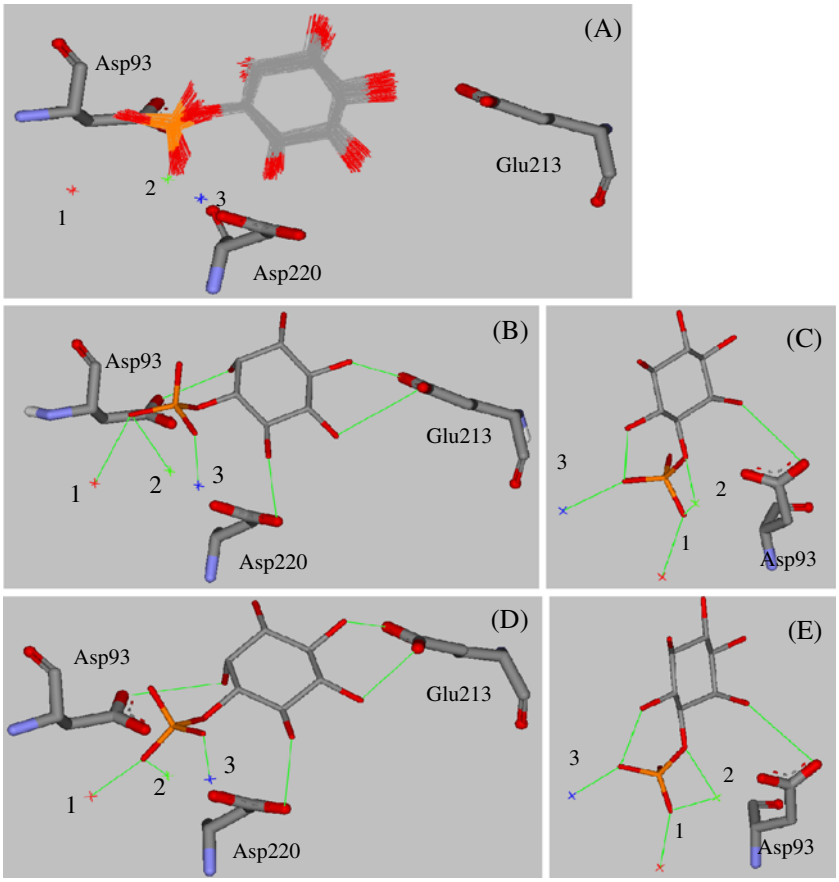

Fig. 2 The docking result in human IMPA1. *Myo*-inositol 1-phosphate docked in the active cavity of human IMPA1. The enzyme is represented by stick and the substrate by line. **a)** Superimposition of 83 docking results. **b)** The docked results showing the coordinates among the phosphate group and three Ca^{2+} ions, and the hydrogen bonds between inositol ring and the enzyme. Green line represents the electrostatic interactions or hydrogen bonds. **c)** The docked result showing the OH group vicinal to phosphate moiety interacted with Ca^{2+}-3, and the bridging oxygen atom with Ca^{2+}-2; **d)** and **e)** The docking manners observed in the crystal structures of the human IMPA1/*myo*-inositol 1-phosphate complex

human IMPA2. As described in the methods, we added three Mg^{2+} ions to the crystal structure of metal-ion free human IMPA2. Mg^{2+}-1 was located within 3 Å from the carboxylate of Glu81 (corresponding to Asp70 human IMPA1) and Asp101 (Asp90 of human IMPA1), and the carbonyl of Ile103 (Ile92 of human IMPA1). Mg^{2+}-2 was located within 3 Å of the carboxylates of Asp101, Asp104, and Asp231 (Asp220 of human IMPA1). Mg^{2+}-3 was bound to the carboxylate of Glu81.

Table 1 The free energy changes in the docking of the substrates to human IMPA1 and 2. The substrate-docking was repeated 200 times per compound and the average of free energy changes and their deviations were calculated as described in the methods

Substrate	AutoDock energy (ΔG: kcal/mol)		
	IMPA1	IMPA2-3 Mg	IMPA2-2 Mg
myo-inositol-1P	-12.10±0.14	-12.00±0.17	-11.16±0.44
myo-inositol-2P	-12.10±0.34	-12.08±0.42	-10.69±0.16
myo-inositol-3P	-12.30±0.11	-12.25±0.11	-10.86±0.09
myo-inositol-4P	-12.88±0.50	-12.78±0.33	-10.26±0.12
myo-inositol-5P	-12.43±0.14	-12.35±0.23	-10.17±0.13
myo-inositol-6P	-12.12±0.09	-12.07±0.10	-10.89±0.25
2′-AMP	-13.29±0.21	-12.97±0.50	-11.29±0.15
ADP	-15.87±1.11	-14.36±2.29	-13.10±1.27
FDP	-13.86±0.60	-13.06±0.77	-11.44±0.58

The docking study with this template showed that *myo*-inositol 1-phophate docked to the IMPA2 with an average ΔG value of -12.0 kcal mol^{-1} and the deviation was 0.17 (Table 1). The docking patterns varied to a slight extent more inconsistently than those of the IMPA1, but in 61 of 200 docking results, the conformations of enzyme-substrate complex were overlapped significantly (Fig. 3a). The r.m.s. deviations of phosphorus atom and C4 were 0.17 and 0.39 Å, respectively.

The docking manner was that the non-bridging oxygen atoms O8 and O9 coordinated three Mg^{2+} ions, and the 2-OH and 4-OH groups of inositol ring formed hydrogen bonds with Asp104 and Gln224, respectively (Fig. 3b). Moreover, the 6-OH group was shown to form a hydrogen bond with Asp231, and close to the phosphate oxygen O9 (within 3 Å), which coordinated Mg^{2+}-3 (Fig. 3c).

The docking study on other *myo*-inositol monophosphates, which have been known to be substrates for the IMPA1 and 2, showed that each substrate formed its own docking manner, while including common docking features. That is, the non-bridging oxygen atoms of the phosphate moiety coordinated three Mg^{2+} ions. Further-

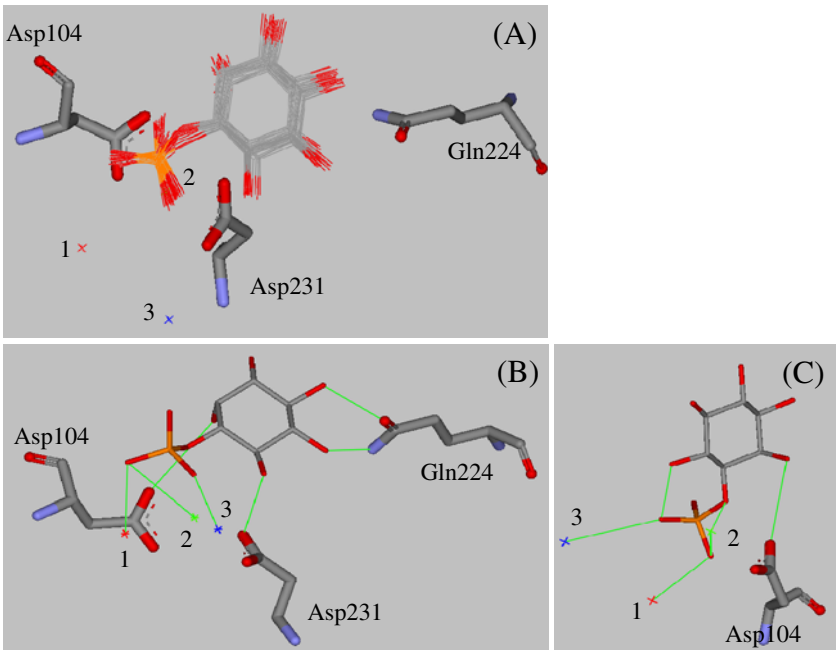

Fig. 3 The docking results of *myo*-inositol 1-phosphate to human IMPA2. *Myo*-inositol 1-phosphate docked in the active cavity of human IMPA2. **a**) Superimposition of 61 docking results. **b**) The human IMPA2/*myo*-inositol 1-phosphate docking model. The phosphate moiety coordinated three Mg^{2+} ions. The inositol rings formed hydrogen bonds with Asp104, Gln224 and Asp231. **c**) Interactions of the non-bridging oxygen O9 and the bridging oxygen O1 with the 2-OH group and Mg^{2+}-2, respectively

more, except *myo*-inositol 2-phosphate, these substrates formed more than three hydrogen bonds between the inositol ring and the ligands in the active cavity (Asp104, Thr106, Gln224 and Asp231 in IMPA2).

For instance, in the case of *myo*-inositol 5-phosphate, 103 of 200 docking results showed that it formed an electrostatic interaction between the metal ions and phosphate moiety, and the 2-OH group formed a hydrogen bond with the carbonyl group of Gln224, the 3-OH with the nitrogen atom of side chain of Gln224, and 4-OH with Asp231 (Fig. 4a, b). The non-bridging oxygen O9 interacted with the 4-OH group, and the bridging oxygen O1 with Mg^{2+}-2 (Fig. 4c). These results were very similar to those of *myo*-inositol 3-phosphate and 6-phosphate (data not shown).

In the case of *myo*-inositol 4-phosphate, it was shown that the inositol ring docked to the enzyme by forming four hydrogen bonds; the 2-OH group with Asp104, the 3-OH with Asp231, the 5-OH group with Thr106, and the 6-OH with the carbonyl group of main chain of Gly205 (data not shown).

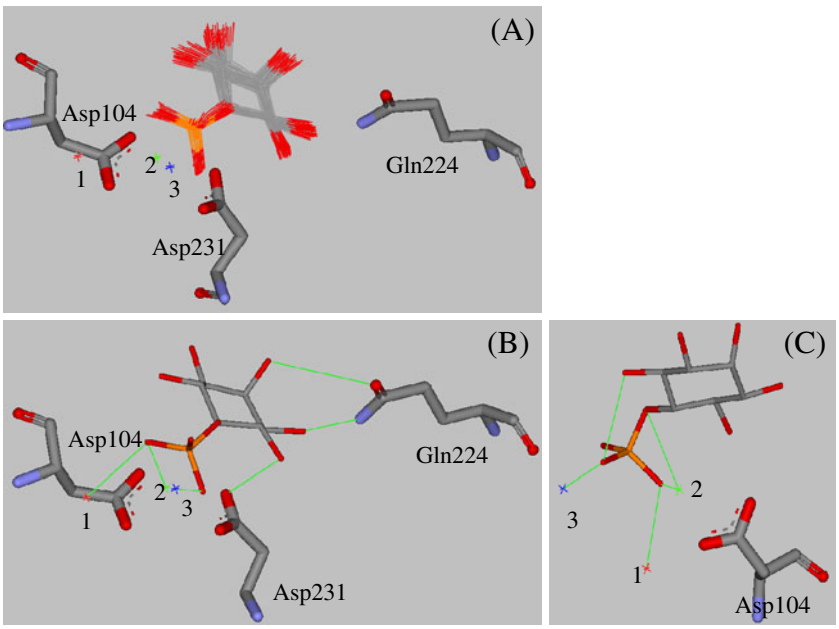

Fig. 4 The docking results of *myo*-inositol 5-phosphate to human IMPA2. *Myo*-inositol 5-phosphate docked in the active cavity of human IMPA2. **a**) Superimposition of 103 docking results. **b**) The human IMPA2/*myo*-oinositol 5-phosphate docking model. The phosphate moiety coordinated three Mg^{2+} ions. The inositol rings formed three hydrogen bonds with Gln224 and Asp231. **c**) Interactions of the non-bridging oxygen O9 and the bridging oxygen O1 with the 4-OH group and Mg^{2+}-2, respectively

As mentioned above, each *myo*-inositol monophosphate had its own binding manner, but they showed common binding patterns; the non-bridging oxygen atom O9 coordinated Mg^{2+}-3 and O8 coordinated both Mg^{2+}-1 and Mg^{2+}-2. The bridging oxygen atom coordinated Mg^{2+}-2. Moreover, more than three OH groups of the inositol ring formed hydrogen bonds with the residues Asp104, Thr106, Gln224 or Asp231 in IMPA2. Three hydrogen bonds can stabilize the binding of the inositol ring to IMPA2.

On the other hand, in the case of *myo*-inositol 2-phosphate, only two hydrogen bonds were formed between the inositol ring and the enzyme. The 3-OH group bound to Asp104 and the 5-OH to Gln224 (Fig. 5a, b). However, the distance between the 1-OH group and Asp231 was more than 6 Å (Fig. 5b). Furthermore, although all the other substrates showed the OH group vicinal to the phosphate group interacted with the non-bridging oxygen O9 at a distance of less than 3.5 Å, the distance between 1-OH of *myo*-inositol 2-phosphate and the O9 was more than 4.5 Å (Fig. 5c). Probably, as the 1-OH group of *myo*-inositol 2-phosphate is at an axial position of the inositol ring, the distance to O9 was more than 4 Å. The OH group vicinal to the phosphate group is required to form an intramolecular interaction with the phosphate oxygen atom, because it plays an important role by forming the pentavalent phosphorus transition state [11, 25, 26]. These results suggest that the binding of *myo*-inositol 2-phosphate to the IMPA2 is unstable and it is not easy to induce a trigonal bipyramidal structure. This may explain why *myo*-inositol 2-phosphate is a weaker substrate than other *myo*-inositol monophosphates.

The docking of the substrates to the IMPA2 which formed a complex with two Mg^{2+} ions showed that *myo*-

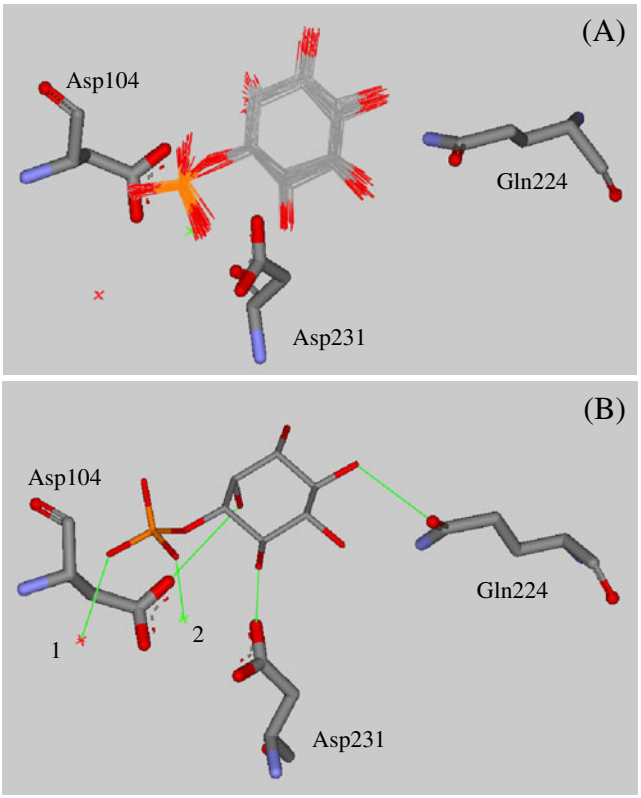

Fig. 6 The docking results in the two Mg^{2+}-ion-bound human IMPA2. The substrate *myo*-inositol 1-phosphate represented as docked to the two Mg^{2+}-ion- bound human IMPA2. **a**) Superimposition of 38 results. **b**) The human IMPA2/*myo*-inositol 1-phosphate docking model. The phosphate moiety coordinated two Mg^{2+} ions. The inositol rings formed three hydrogen bonds with Asp104, Gln224 and Asp231

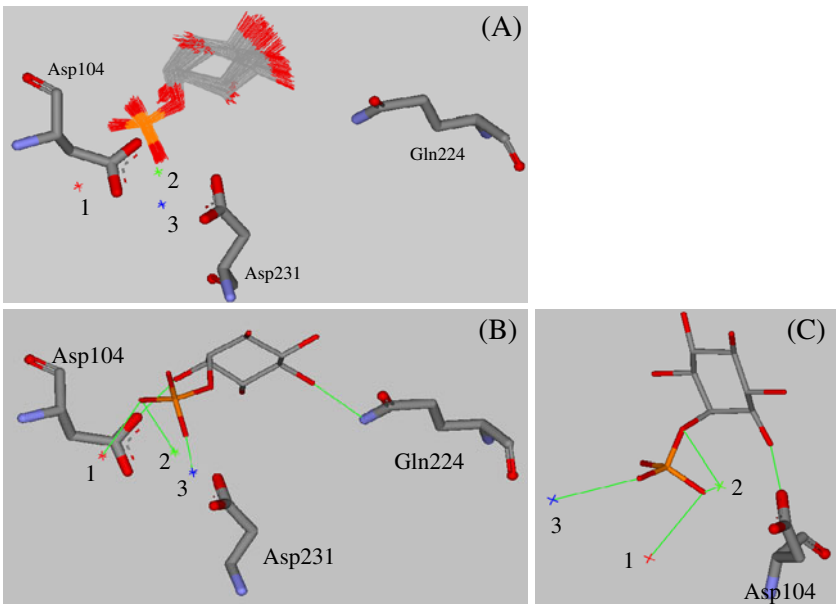

Fig. 5 The docking models of *myo*-inositol 2-phosphate to human IMPA2. *Myo*-inositol 2-phosphate docked in the active cavity of human IMPA2. **a**) Superimposition of 120 docking results. **b**) The human IMPA2/*myo*-inositol 2-phosphate docking model. The phosphate moiety coordinated three Mg^{2+} ions. The inositol rings formed two hydrogen bonds with Asp104 and Gln224. **c**) Interactions of the bridging oxygen O1 with Mg^{2+}-2, but non-interaction between the 1-OH group and O9

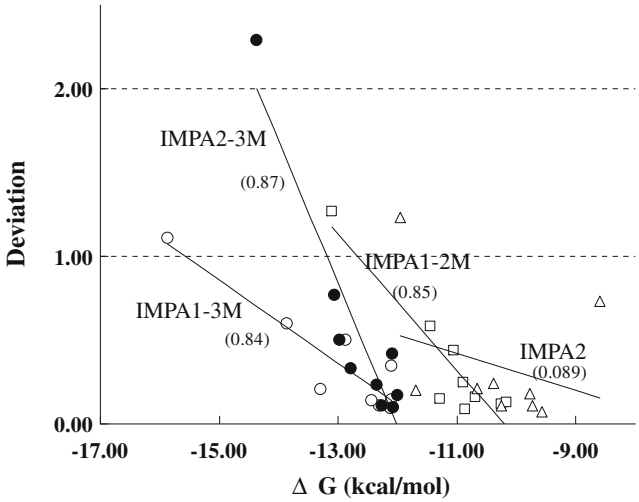

Fig. 7 Relationship between ΔG values and their standard deviation values. The ΔG values are plotted against their deviation values. ○; the docking results in hman IMPA1, ●;in the three Mg^{2+}-ion-bound human IMPA2, □;in the two Mg^{2+}-ion-bound human IMPA2, and △;in the metal ion free human IMPA2. Each line represents a linear relationship between ⊿G value and deviation and each R^2 value is in parents

inositol 1-phosphate docked to the IMPA2 with a ΔG value of about -11 kcal mol^{-1} and the deviation was 0.44 (Table 1). The docking patterns varied very inconsistently, but 38 of 200 docking results were similar (Fig. 6a). That is, the non-bridging oxygen atoms O8 and O9 coordinated Mg^{2+}-1 and Mg^{2+}-2, respectively, and the 2-OH, 4-OH and 6-OH groups of the inositol ring formed hydrogen bonds with Asp104, Gln224 and Asp231, respectively (Fig. 6b). However, due to a lack of interaction between the non-bridging oxygen of the phosphate group and the third Mg^{2+} ion (Fig. 6b), the IMPA2 and *myo*-inositol 1-phosphate complex could not induce the transitional state, i.e., bipyramidal structure [11, 25].

There were other docking patterns in the 200 results, but they commonly showed that the phosphate moiety was distant from the metal ions. In these cases, the non-bridging oxygen atoms O8 and O9 interacted with Cys107 and Arg202 (and/or Arg178) in the cavity and the distances between phosphate moiety and metal ions were more than 5 Å (data not shown). Since the two-metal-ion bound IMPA2 was crystallized, the two-ion bound IMPA2/substrate complexes, which are inactive, could be formed in vivo.

The average ΔG values were increased by changing the number of metal ion in the IMPA2. When the structure of IMPA2 forming a complex with three Mg^{2+} ions was used, the ΔG values of *myo*-inositol monophosphates were plotted at nearly -12 kcal mol^{-1} and the standard deviation values were less than 0.5. However, when we used the two-Mg^{2+}-ion bound model, the plots of ΔG values shifted to right and the deviations were less than 0.5. When the metal-ion free structure was used as a template, the ΔG values were plotted between -10 and -9 kcal mol^{-1} and the deviations were less than 0.4 (Fig. 7). The non-substrate compounds, ADP and FDP docked to the IMPAs with similar ΔG values of *myo*-inositol monophosphates. However, the deviation values were significantly larger than those of *myo*-inositol monophosphates, indicating that these compounds were docked inconsistently to the IMPAs.

Taken together, we propose that the binding manner of *myo*-inositol 1-phosphate in the three-metal-ion bound human IMPA2 is almost the same as that of the human IMPA1/*myo*- inositol 1-phosphate complex, as well as bovine IMPA-inositol 1-phosphate complex. The human IMPA2/*myo*-inositol 1-phosphate docking model is likely to form the transitional state, trigonal bipyramidal structure, suggesting that human IMPA2 proceeds the dephosphorylation reaction through the three-metal-ion mechanism rather than two-metal-ion.

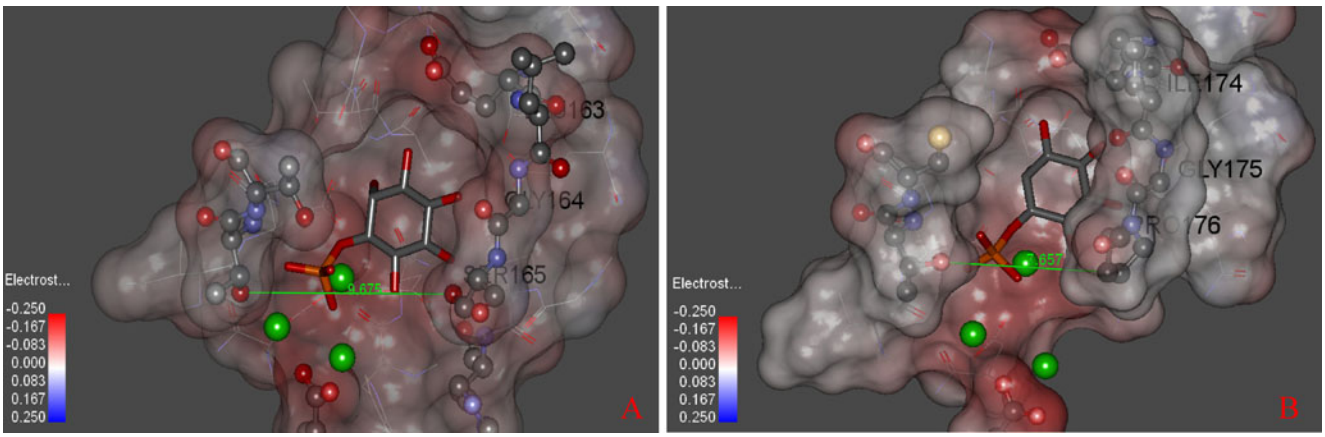

Fig. 8 Electrostatic surfaces of the substrate binding pockets in IMPA1 and 2. All residues within 5 Å of docked *myo*-inositol 1-phosphate and metal ions are represented. The electrostatic representations were obtained by DS modeling using a dielectric constant 4, and are colored by calculated charge from red to blue. A; IMPA1, B; IMPA2

Although the enzyme-substrate complexes were similar to each other, the enzymatic activity in vitro is significantly higher in IMPA1 than in IMPA2. This discrepancy can not be explained by the present study. However, as can be seen in Fig. 8, the architecture consisting of Ile174, Gly175 and Pro176 covers the substrate binding site in the catalytic pocket of IMPA2, while the corresponding residues Gln163, Gly164, and Ser165 do not cover the pocket in IMPA1. The narrowest distance between the two atoms in the IMPA2 pocket is 7.66 Å, while it is 9.68 Å in IMPA1 (Fig. 8). Since the three-peptide forms a cap that partially hinders the substrate binding region, *myo*-inositol monophosphate may have more difficulty accessing the binding site in IMPA2 than IMPA1. This structural difference may reflect the substrate selectivity in these two enzymes. The difference caused by the steric hindrance cannot be accounted for in the docking study, because computation with the substrates placed on the grid center eliminates the necessity to include steric hindrance. Although the docking results were not able to distinguish the substrate selectivity between the two enzymes, these structural difference near the substrate binding sites may explain the lower activity of IMPA2.

Furthermore, Ohnishi et al. has reported that the affinity of Mg^{2+} to human IMPA2 is lower than that of human IMPA1. IMPA1 is inhibited by Mg^{2+} at higher concentrations, while IMPA2 is not [15]. These biochemical differences indicate the two enzymes possess each metal-ion-ligand chelating circumstance in their cavities. Moreover, in the IMPA-catalyzed reaction, water molecules play a very important role to initiate hydrolysis of phosphate ester. Especially the third metal ion consists of a single protein ligand and five water molecules in the bovine IMPA crystal [11]. Therefore, we need more information about the water molecules (and third ion) in the structure of IMPA2 crystal to have a more precise investigation. In addition, the precise positions of three Mg^{2+} ions should be confirmed by further molecular dynamics calculations and we are currently working on this problem.

Since lithium inhibits IMPA and modulates phosphatidylinositol cell signaling at therapeutically relevant concentrations (0.5-1.0 mM), the human IMPA2 has attracted attention as a molecular target in the treatment of bipolar disorder [26–30]. In order to develop a noble lead compound, we consider that both two-metal- and three-metal-ion-bound forms of IMPA2 can be used. For example, an inhibitor which maintains a stable structure of the two-metal-ion-bound form by binding to the residue such as Cys107 that does not exist in the IMPA1, can be conceivable. On the other hand, as can be seen in Fig. 8, IMPA2 possesses a cap structure near the three metals but IMPA1 does not, suggesting this region can be a binding site of an inhibitor. Therefore, based on our present results obtained by AutoDock with both two-metal- and three-metal-ion bound models, we hope that a noble lead compound can be developed for the therapy of bipolar disorder.

Acknowledgments We thank Dr. E. Cooper at Ritsumeikan University for his helpful suggestions concerning the manuscript.

References

1. Nothen MM, Cichon S, Rohleder H, Hemmer S, Franzek E, Fritze J, Albus M, Borrmann-Hassenbach M, Kreiner R, Weigelt B, Minges J, Lichtermann D, Maier W, Craddock N, Fimmers R, Holler T, Baur MP, Rietschel M, Propping P (1999) Mol Psychiatry 4:76–84
2. Yoshikawa T, Turner G, Esterling LE, Sanders AR, Detera-Wadleigh SD (1997) Mol Psychiatry 2:393–397
3. Ohnishi T, Yamada K, Ohba H, Iwayama Y, Toyota T, Hattori E, Inada T, Kunugi H, Tatsumi M, Ozaki N, Iwata N, Sakamoto K, Iijima Y, Iwata Y, Tsuchiya KJ, Sugihara G, Nanko S, Osumi N, Detera-Wadleigh SD, Kato T, Yoshikawa T (2007) Neuropsychopharmacology 32:1727–1737
4. Sjoholt G, Ebstein RP, Lie RT, Berle JO, Mallet J, Deleuze JF, Levinson DF, Laurent C, Mujahed M, Bannoura I, Murad I, Molven A, Steen VM (2004) Mol Psychiatry 9:621–629
5. Atack JR (1996) Brain Res Rev 6:183–190
6. Parthasarathy L, Vadnal RE, Parthasarathy R, Devi CS (1994) Life Sci 54:1127–1142
7. Nakayama J, Yamamoto N, Hamano K, Iwasaki N, Ohta M, Nakahara S, Matsui A, Noguchi E, Arinami T (2004) Neurology 63:1803–1807
8. Arai R, Ito K, Ohnishi T, Ohba H, Akasaka R, Bessho Y, Hanawa-Suetsugu K, Yoshikawa T, Shirouzu M, Yokoyama S (2007) Proteins 67:732–742
9. Greasley PJ, Gore MG (1993) FEBS Lett 27:114–118
10. Greasley PJ, Hunt LG, Gore MG (1994) Eur J Biochem 222:453–460
11. Gill R, Mohammed F, Badyal R, Coates L, Erskine P, Thompson D, Gore Cooper J, Wood S (2005) Acta Crystallogr D Biol Crystallogr 61(Pt 5):545–555
12. Ganzhorn AJ, Rondeau JM (1997) Protein Eng 10:61–70
13. Ganzhorn AJ, Lepage P, Pelton PD, Strasser F, Vincendon P, Rondeau JM (1996) Biochemistry 35:10957–10966
14. Pollack SJ, Atack JR, Knowles MR, McAllister G, Ragan CI, Baker R, Fletcher SR, Iversen LL, Broughton HB (1994) Proc Natl Acad Sci USA 91:5766–5770
15. Ohnishi T, Ohba H, Seo KC, Im J, Sato Y, Iwayama Y, Furuichi T, Chung SK, Yoshikawa T (2007) J Biol Chem 282:637–646
16. Brown AK, Meng G, Ghadbane H, Scott DJ, Dover LG, Nigou J, Bersa GS, Futterer K (2007) BMC Struct Biol 7:55
17. Wang Y, Stieglitz KA, Bubunenko M, Court DL, Stec B, Roberts MF (2007) J Biol Chem 282:26989–26996
18. Tabata K, Baba K, Shiraishi A, Ohno T, Ito M, Fujita N (2007) Biochem Biophys Res Commun 363:861–866
19. Murakami M, Shiraishi A, Tabata K, Fujita N (2008) Biochem Biophys Res Commun 371:707–712
20. Morris GM, Goodsell DS, Huey R, Olson AJ (1996) J Comput Aided Mol Des 4:293–304
21. Nonaka Y, Hiramoto T, Fujita N (2005) Biochem Biophys Res Commun 337:282–288

22. Hallcher LM, Sherman WR (1980) J Biol Chem 255:10896–10901
23. Jackson RG, Gee NS, Ragan CI (1989) Biochem J 264:419–422
24. Miller DJ, Beaton MW, Wilkie J, Gani D (2000) Chembiochem 1:262–271
25. Attwood PV, Ducep JB, Chanal MC (1988) Biochem J 253:387–394
26. Atack JR, Broughton HB, Pollack SJ (1995) FEBS Lett 361:1–7
27. Harwood AJ (2005) Mol Psychiatry 10:117–126
28. Agam G, Bersudsky Y, Berry GT, Moechars D, Lavi-Avnon Y, Belmaker RH (2009) Biochem Soc Trans 37:1121–1125
29. Belmaker RH, Bersudsky Y (2009) Neurosci Biobehav Rev 31:843–849
30. Ohnishi T, Watanabe A, Ohba H, Iwayama Y, Maekawa M, Yoshikawa T (2010) Neurosci Res 67:86–94